Motion-compensated Multi-dimensional RF Excitation Pulses

K. Nehrke[1], P. Börnert[1]
[1]Philips Research Laboratories, Hamburg, Germany

Introduction:
Multi-dimensional RF pulses can be used in a variety of different applications. To overcome their problems related to off-resonance, limited spectral bandwidth and limitations caused by the finite lifetime of transverse magnetization, RF pulse segmentation has been proposed [1]. An RF pulse can be subdivided into a number of interleaves, each subsampling the excitation k-space while a corresponding B_1 waveform is applied. The individual sub-RF pulses are shorter, more robust and their spectral bandwidth is increased. This enables the excitation/refocusing of any desired spatial profile, but its final spatial definition is achieved via signal averaging of their corresponding MR data (Fig.1). This averaging process makes these segmented RF pulses prone to inter-pulse motion resulting in a blurred excitation profile and an incomplete cancellation of the aliasing artefacts, which degrades pulse performance. This hampers e.g. their application in cardiac MRS, where the localization of a volume of interest (VOI) is impeded by respiratory and cardiac motion. The present work shows a new approach to overcome this problem by prospectively correcting segmented RF excitation pulses for affine motion.

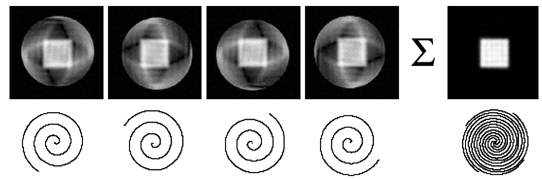

Figure 1: Pinwheel excitation pulse subdivided into four excitation segments (top row: spatial excitation profile, bottom row: k-space trajectory interleaves).

Methods:
As recently shown, motion described by affine transformations (rotation, stretching, shear and translatory motion) can be corrected prospectively for arbitrary imaging sequences during signal excitation and reception as well [2]. This is achieved by appropriate tuning of the sequence parameters: insertion of Eqs. 2-4 (Fig.2) into the Bloch equations formally removes the time variance of the position vector (Eq. 1). Thus, the patient-specific prospective correction of affine motion described in [2] can be extended to multidimensional excitation pulses. This approach has been fully integrated on a clinical scanner platform (Philips ACHIEVA) equipped with a real-time capable spectrometer. Experiments were carried out on a moving resolution phantom, which performed a continuous oscillatory rotating motion (rotation amplitude: 30°, period: 4s). A square-shaped excitation target was chosen (Fig.3), which corresponds to a 2D-sinc-shaped RF pulse sampled along a spiral excitation trajectory. The pulse was interleaved in four excitations, which was realized by rotating the gradient coordinate systems by multiples of 90° (cf. Fig.1). The AM pulse shape was kept constant for the different interleaves according to the fourfold symmetry of the chosen target profile. To compensate for the actual rotation angle of the moving phantom, a real-time rotation was applied to the gradient coordinate system. Furthermore, the off-centre position of the rotation axis with respect to the gradient centre led to an additional translatory component x in the rotated coordinate system, which was corrected by real-time modulation of the FM waveform according to the relation $fm(t) = \gamma G(t) \cdot x$. The correction parameters were provided by a real-time pencil beam navigator applied prior to the excitation pulse (5 ms delay) using a motion model calibrated in a pre-scan [2]. The navigator was positioned through an appropriate section of the phantom providing sufficient contrast variation for monitoring motion. To evaluate the performance of the motion compensated pinwheel excitation, the pulse profile was imaged. Four averages were performed according to the four spiral interleaves of the excitation pulse. The images were compared to experiments, where the phantom was resting, or the motion correction was turned off.

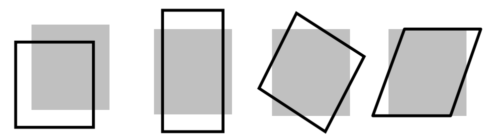

$$\mathbf{r}(t) = \mathbf{A}(t) \cdot (\mathbf{r}' + \mathbf{r}_0(t)) \quad (1)$$

$$\mathbf{G}(t) = {}^{t}\mathbf{A}^{-1}(t) \cdot \mathbf{G}'(t) \quad (2)$$

$$B_1(t) = B'_1(t) \cdot \exp(-i\gamma \int_0^t \mathbf{G}'(\tau) \cdot \mathbf{r}_0(\tau)\, d\tau) \quad (3)$$

$$M_{xy}(t) = M'_{xy}(t) \cdot \exp(-i\gamma \int_0^t \mathbf{G}'(\tau) \cdot \mathbf{r}_0(\tau)\, d\tau) \quad (4)$$

Figure 2: Affine motion (top row and Eq.1) can be precompensated by adapting gradient, transmitter and receiver waveforms (Eqs.2-4).

Results:
For the resting phantom, a well-shaped square excitation profile was observed (cf. Fig. 3d). In case of motion, severe ghosting and blurring artefacts arose, if no motion correction was applied (cf. Fig. 3e). In contrast, prospective motion correction provided image quality almost identical to the case without any motion (cf. Fig. 3f).

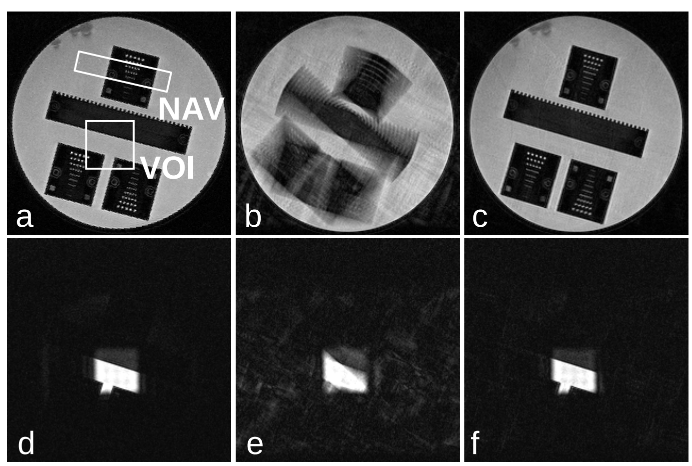

Figure 3: Quality phantom imaged with conventional slice selection (top row) and 2D spatial localization pulse (bottom row). Images are shown for a resting phantom (left column) and moving phantom (middle/right column: w/o prospective motion correction. Each interleave consisted of a 5-turn spiral covering three lobes of a 2D-sinc pulse. In (a) the position of the square-shaped VOI (40 x 40 mm²) and the pencil beam navigator steering the motion correction are marked with white boxes.

Discussion and Conclusion:
This work demonstrates that patient-specific correction of affine motion is feasible on a clinical scanner even for complicated excitation pulses like segmented 2D spiral excitation despite the complexity of the approach. Thus, this technique may be useful for spectroscopic applications, where cardiac and/or respiratory motion impedes spatial localization.

References:
[1] Hardy et al. Magn Reson Med 1991; 17: 315-327.
[2] Manke et al. Magn Reson Med. 2003; 50(1):122-31.